



# Evaluation of groundwater repositories in parts of Enugu, Eastern Nigeria via electrical resistivity technique

Mirianrita Ngozi Ossai<sup>1</sup> · Francisca Nneka Okeke<sup>1</sup> · Daniel Nnaemeka Obiora<sup>1</sup> · Johnson Cletus Ibuot<sup>1</sup>

Received: 7 August 2021 / Accepted: 29 November 2022 / Published online: 16 January 2023  
© The Author(s) 2023

## Abstract

Resistivity survey was carried out in Enugu North, Southeastern Nigeria, in order to evaluate the groundwater condition of the area. The inadequacy of surface water, proper knowledge of the aquifer and increasing population has affected the extraction and development of groundwater in the area. Resistivity, thickness, depth, curve frequencies and protection level were determined. The result revealed a total of 5–6 geoelectric layers with model curves exhibiting the following curve types: KHK taking about 10%; AAKQ, KHAK, KHAA, HKQ, HKQQ and HAA taking 12%, AAA, AKH, HAK and KHKQ taking 24% while AKQ and AAK take 20 and 34%, respectively. The aquifer is within the fourth and fifth layer considering the layer with the largest thickness with the fourth layer taking up to 84% of the aquifers in the study area. The overburden layer resistivity and thickness ranged from 589.8 to 85,094.8  $\Omega\text{m}$  and 8.9 to 99.5 m with mean values of 42,642.3  $\Omega\text{m}$  and 54.2 m, respectively. The contour maps were generated using Surfer software package version 15 which show the variation of overburden parameters. The study area was generally considered as having a high protective level as a result of the low values of geophysically based protection index of the aquifer layers and weak to fair GPI rating implying that the aquifer can be protected from infiltrating contaminants. However, high hydraulic conductivity and porosity suggest high groundwater potential and high infiltration of polluted geofluids.

**Keywords** Electrical resistivity · GPI · Corrosivity · Aquifer unit · Permeability

## Introduction

The study area lacks abundant surface water resources resulting to increase the demand for groundwater (Uguwanyi et al. 2015; Ossai et al. 2020). Insufficient knowledge of the aquifer nature of the subsurface materials limits groundwater development in the area which is important for borehole construction and in several cases has resulted in unproductive boreholes, extremely low yield, total failure of some boreholes in the area and risk of spending large sum of money in sinking boreholes that will eventually be unsuccessful. Poor quality of water resources does not only affect the environment and socio-economic activities but the health of the populace (risk of water related diseases). Unsafe water is one of the major factors attributed to about 88% of death due

consumption of polluted groundwater which results in water related diseases such as diarrhea (UNICEF 2006; Black et al. 2003). Globally water related diseases kill around 525,000 children under the age of 5 (WHO 2008, 2017) thus the need to crave for safe and clean water arises.

Tremendous increase in population has increased industrialization, urbanization and indiscriminate dumping sites yielding contaminated plumes which when percolated into the aquifer layers renders it unsuitable for human consumption (Ibuot et al. 2017a, b). Although, groundwater generally is naturally protected from contamination, it can be unsafe owing to the susceptibility of its protective layers (McDonald et al. 2005). Substantial amount of money will be needed to clean up groundwater once it is contaminated, but most times it is not feasible to achieve clean up within a reasonable time frame (Talabi & Kayode, 2019; Ossai et al. 2020) because replacing contaminated sources with potable sources like treated bottled water are costly and non-comparable to that of existing ground water resources (Abdalla 1990). Notwithstanding that pumping test method is good in evaluating aquifer characteristics; it is capital intensive

✉ Mirianrita Ngozi Ossai  
rita.ossai@unn.edu.ng

<sup>1</sup> Department of Physics and Astronomy, Faculty of Physical Sciences, University of Nigeria, Carver Building, 1 University Road, Nsukka 410001, Enugu State, Nigeria

and consumes much time. However, the results from Shingal and Niwas (1985) indicate that the DC resistivity method provide a fast, less expensive and noninvasive way to study aquifers.

There is a need for geophysical study in this area in order to understand the true nature of the aquifer repositories, delineate areas with good protective layers and possible contamination source for effective groundwater exploration, exploitation and management. Electrical resistivity method is one of the best tools in geophysical investigation used for site investigation toward the determination of overburden resistivity and thickness (Kearey and Brooks 1991). Many authors proved that in order to achieve long lasting boreholes and sustainable supply of water, electrical resistivity survey should be carried out so as to identify groundwater prospective potential and good protective capacity zones for groundwater exploitation (Ezeh et al. 2012; Ugwuanyi et al. 2015; Mallums et al. 2019; Obiora and Ibuot, 2020; Ossai et al. 2020; Ochuko et al. 2021). The significance of using resistivity method in geological terrains to delineate subsurface geological structures, aquifer layers and types of aquifer, thickness and depth extent is successful because of the correlation that exists between electrical properties, geologic formations and fluid contents (Ossai et al. 2020). In groundwater exploration, the vertical electrical sounding (VES) technique is commonly used due to its proneness to near surface lateral inhomogeneities and extraneous current (stray/telluric currents), greater probing depth, well developed and more diversified interpretation techniques, lesser time and its simplicity to determine the variation of the subsurface geomaterials.

The estimation of the geophysically based protection index (GPI) which is used for quantification of aquifer vulnerability have been employed successfully by researchers to delineate areas that have poor protection level hence vulnerable to pollution (Rottger et al. 2005; Casas et al. 2008). Resistivity of most rocks depends on moisture content in their pores, geometry of these pores and the salinity of the water (Todd 1980). Researchers have reported that groundwater quality is majorly affected by percolation of pollutants into aquifer zones (George et al. 2013; Ibuot et al. 2017a, b, 2019a) which is also hugely controlled by the characteristics of the aquifer/overlying layers, recharge-discharge rate and the type of pollutants. The impact of pollutants on groundwater quality has been assessed and results from various works revealed high conductivity of polluted aquifer as evident from the works of (Ugwu and Nwosu 2009; Omongunloye and Jimoh 2013; Ganiyu et al. 2015 and Ibuot et al. 2019a). The electrical conductivity of some pollutants is often much higher than that of natural groundwater, and this large gap in their electrical conductivity value enables contaminated plumes to be detected using geophysical methods. Vertical electrical sounding (VES) is a noninvasive method

that helps in understanding aquifer hydrogeological behaviors and revealing contaminant zones due to the conductive nature of most pollutants (Pomposiello et al. 2012, Ekanem, 2020; Ibuot et.al. 2020; Thomas et al. 2020). The subsurface properties affect the withdrawal and flow of groundwater which depends on the formation pore connectivity, pore angularity, compaction, pore-grain volume ratio, resistivity and heterogeneity of formations (George et al. 2017; Ibuot et al. 2019b; Ibuot and Obiora 2021). This research employed electrical resistivity technique to investigate and characterize the aquifer repository, protective capacity of the aquifer overlying layers using GPI and subsurface properties that influence the flow of groundwater.

### Location and geology of the study area

The study area is guinea-savanna vegetation located within the Anambra Sedimentary Basin of the Lower Benue Trough covering Nsukka, Igbo-Eze north, Igbo-Eze south and parts of Udenu Local Government Areas of Enugu State. The study area lies between latitudes  $6^{\circ} 8' N-7^{\circ} 03' N$  and longitudes  $7^{\circ} 15' E-7^{\circ} 31' E$ . It has common boundaries with Kogi State, Benue State, Uzo-uwani, Igbo-etiti and Isi-uzo with approximately  $3961 \text{ km}^2$  total surface area (Fig. 1). There is an increasing population of 894,682 at 2006 census to 1,207,200 projected 2016 censuses,<sup>1</sup> which increased the quest for safe water supply, affect water supply availability, water demand patterns and need for proper knowledge of the subsurface geology (Duan and Kaoru 2020). This area of study is accessible through a network of major (Federal highway) and minor roads in addition to several foot paths. The geologic rocks in this area are the Upper Cretaceous in age mainly the upper Nsukka Formation and the underlying Ajali Sandstone which are dominant within the study area (Fig. 2). The two major landforms in this area are the geomorphic residual hills and dry valleys which occur as a result of weathering and differential erosion of clastic materials which are remnant of Nsukka Formation. The residual hills sometimes form outliers on the Ajali Sandstone and are capped by thick deposit of red earth materials and laterite which are permeable, particularly those of Ajali Sandstone thereby allowing easy water percolation into the groundwater table. The Ajali Sandstone consists of thick friable, poorly sorted, coarse-medium grained cross-bedded sandstone of Maastrichtian age (Omeje et al. 2021). Nsukka Formation has a significant groundwater potential and harbors a number of low to moderate yield wells in Nsukka areas due to formation of perched aquifer in Nsukka areas. Eroded remnants of this formation constitute outliers and

<sup>1</sup> National Population Commission of Nigeria (web), National Bureau of Statistics (web).

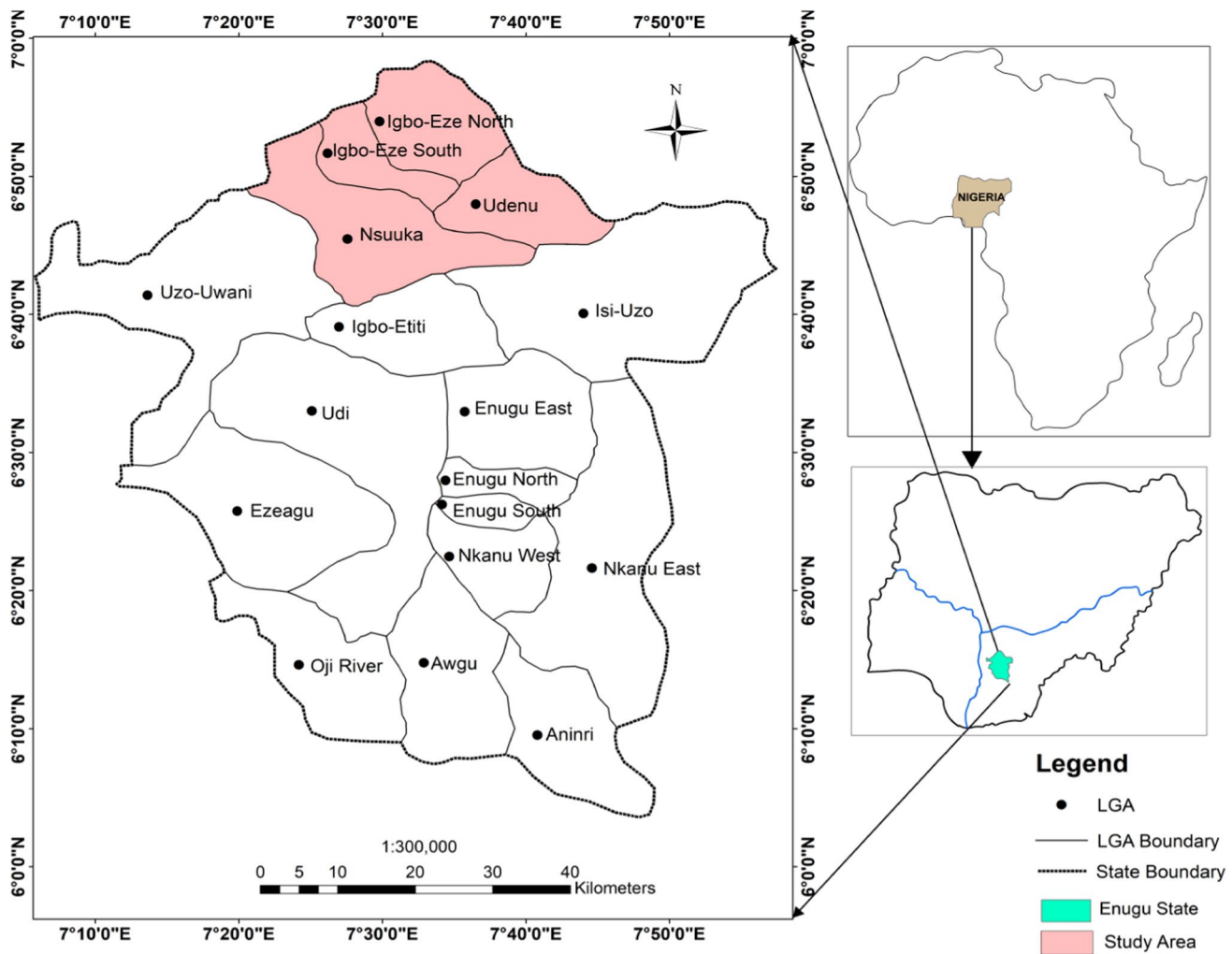


Fig. 1 Map showing the location of the study area

its thickness averages 250 m (Ezeh and Ugwu 2010). The topography is highly undulating with elevation which varies between 281 and 521 m above sea level measured in the field peaked at Umuabo-Ehalumona area at 521 m. Discharge of the existing perched aquifers occur in hilly areas such as Asho hill in Nsukka, Aku hill in Obukpa, Abile hill in Ibagwa-aka and Awula in Ibagwa-Ani.

### Materials and methods

The study involves a total of fifty vertical electrical sounding points carried out using IGIS resistivity meter and its accessories. The survey employed the vertical electrical sounding (VES) with the maximum current electrode separation of 900 m and half potential electrode spacing of 40 m. Also borehole log were obtained from borehole drilling sites close to some VES points. The potential electrodes were expanded symmetrically about a fixed center of spread (Ibuot et al.,

2013; George et al. 2015). The apparent resistivity for this configuration is given by Eq. 1:

$$\rho_a = \pi \cdot \left[ \frac{\left(\frac{AB}{2}\right)^2 - \left(\frac{MN}{2}\right)^2}{MN} \right] \cdot R_a \tag{1}$$

The equation can be simplified to

$$\rho_a = G_s \cdot R_a \tag{2}$$

where  $G_s$  is the geometric factor  $\pi \cdot \left[ \frac{\left(\frac{AB}{2}\right)^2 - \left(\frac{MN}{2}\right)^2}{MN} \right]$  and  $R_a$  is the apparent resistance. where  $AB/2$  and  $MN/2$  are the half current and half potential electrode separations, respectively. The apparent resistivities were computed from the field data using Eq. 2, and the values were plotted on a bi-log-graph having apparent resistivity value against half current electrode spacing. Data filtering and smoothening were carried

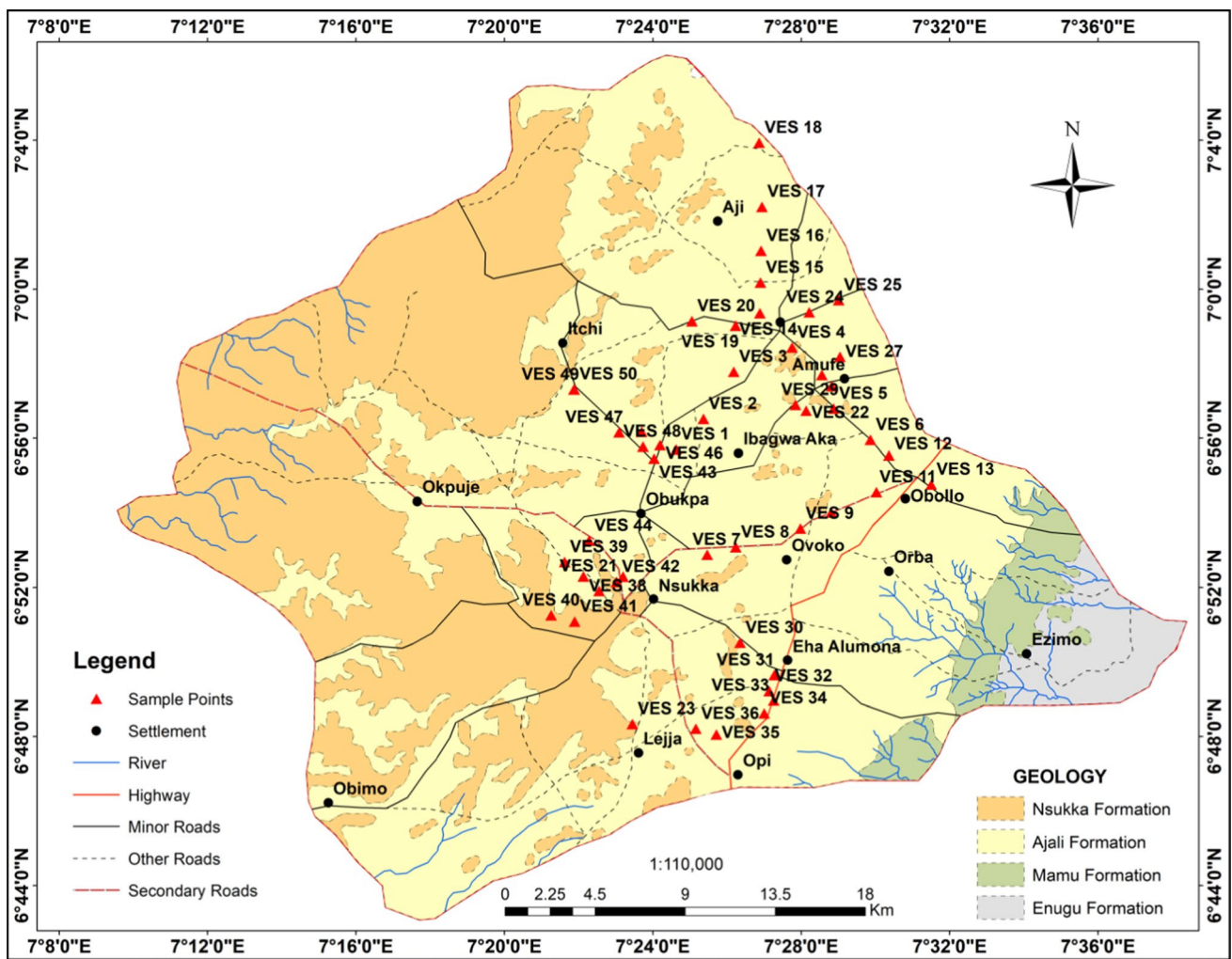


Fig. 2 Map showing the Geology of the study area and sampled VES points

out where necessary to remove traces of noise in the data (Loke 2001). The WINRESIST software program was used in the computer modeling, iteration and curve matching as carefully designed and programmed for Schlumberger array by Zohdy. A good fit with little RMS error was obtained between the field and model curve revealing true values of resistivity, depth, thickness and number of geoelectric layers in Fig. 3. The result of the geoelectric curves revealed 4–6 geoelectric layers as presented in Table 1 and the fourth and fifth layer is found to be associated with larger thickness and was delineated as the water bearing layer (aquifer) in the study area. For better interpretation and understanding of a particular geologic model, it is necessary to combine different parameters such as thicknesses and resistivities of a geoelectric section (Zohdy et al. 1974; Maillet 1947). These principal parameters (resistivity and thickness) are not left out in estimating the hydraulic conductivity, porosity and evaluating geophysically based protection index (GPI). The resistivity model curves for some of the VES stations are

shown in Fig. 3. The resistivities and thicknesses of the layers above the aquifer layer were used to estimate the geophysically based protection index (GPI) which aided in the quantification of aquifer protective capacity. The electrical conductivity ( $\sigma_i$ ) and thickness ( $h_i$ ) were used in estimating the geophysically based Protection Index (Casas et al. 2008) or Integrated Electrical Conductivity, IEC (Rottger et al. 2005). The geophysically based Protection Index (GPI) can be used to assess the aquifer vulnerability using Eqs. 3 and 4;

$$GPI = \sum_{i=1}^n h_i * \sigma_i \tag{3}$$

$$\text{Or } \sum_{i=1}^n h_i * \frac{1}{\rho_i} \tag{4}$$

where  $\sigma_i = 1/\rho_i$ , resistivity ( $\rho_i$ ) and thickness ( $h_i$ ) of each layer above the aquifer are obtained from the inversion of

**Fig. 3** Geoelectric curve for VES 7

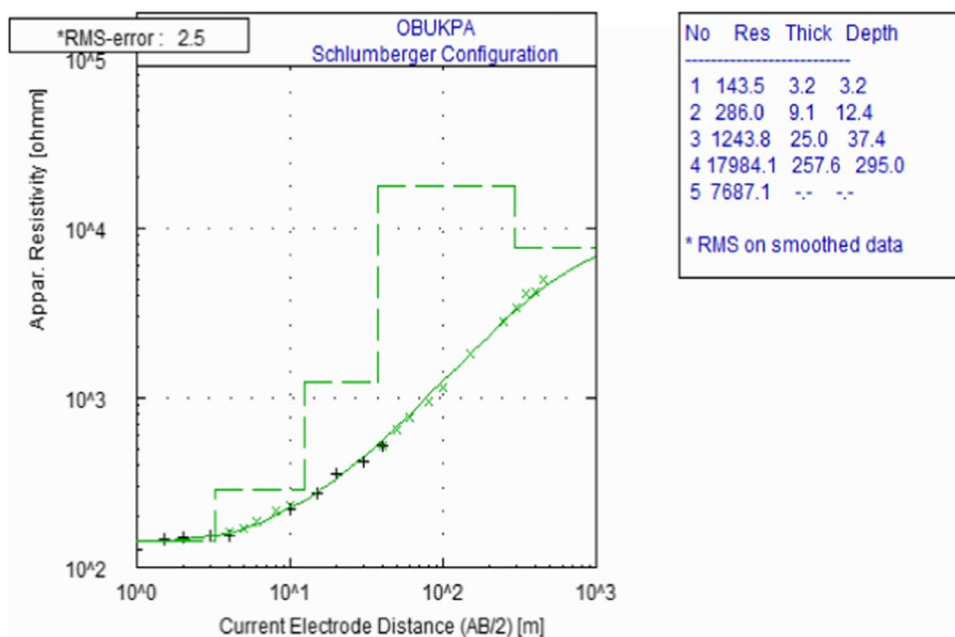


**Table 1** Rating of protective capacity based on GPI (Casas et al. 2008)

Geophysically based protection index (GPI) ( $\Omega^{-1}$ )	Protective capacity rating
> 2.0	Strong
1.1–2.0	Moderate
0.1–1.0	Fair
< 0.1	Weak

resistivity sounding data. The GPI value will have a maximum value when the thickness of low resistivity cap above the aquifer is greater, giving the highest protection level to the groundwater against contamination from the surface (Casas et al. 2008). The rating will be done using Table 1.

The obtained primary parameters (true resistivity and thickness of each layers) from the computer iteration were used to estimate the geohydraulic parameters of the covering layers. Hydraulic conductivity indicates the porous and fractured areas of the subsurface rocks that allow easy movement of groundwater through the pore spaces. It is calculated using Eq. 5 according to Heigold et al. (1979).

$$K = 386.40\rho^{-0.93282} \tag{5}$$

where  $\rho$  is resistivity of the aquifer overlying layers.

Porosity ( $\phi$ ) is the ability of the earth to sieve fluids and is controlled by grain size and shape, degree of rating, extent of cementation and fracturing. The effective

porosity was calculated using the relation from Marotz (1968) expressed as Eq. 6.

$$\phi = 25.5 + 4.5 \ln K \tag{6}$$

where  $K$  is the hydraulic conductivity of the aquifer or overlying layer.

Formation Factor can be expressed in a simplest form as a power law of the effective porosity and geometric factors. An empirical relation, Archie’s Law (Eq. 7) was used to describe this relationship:

$$F = \frac{a}{\phi^m} \tag{7}$$

where  $a$  is pore cementation factor,  $m$  is geometry factor of the pore (empirical constants) and  $\phi$  is effective porosity. Values of  $a$  in the range of 0.47–2.3 can be found in the literature. The value of  $m$  is generally considered to be a function of the kind of cementation present and is reported to vary from 1.3 for completely uncemented soils or sediments to 2.6 for highly cemented rocks, such as dense limestone. For this analysis, values for  $a$  and  $m$  that was used are 0.5 and 1.5, respectively. In addition to the above analysis, the corrosivity of the first layers will be classified and rated based on their resistivity values using Table 2. Corrosivity describes how aggressive water is at destroying or weakening (corroding) pipes and fixtures which causes lead and copper in pipes to leach thus causing rusts and leaks in plumbing pipes and eventually making the groundwater less potable.

**Table 2** Classification of soil resistivity in terms of corrosivity (Baekmann and Schwenk 1975; Agunloye 1984; Oladapo et al. 2004)

Soil resistivity ( $\Omega\text{m}$ )	Soil corrosivity
<10	Very strongly corrosive (VSC)
10–60	Moderately corrosive (MC)
60–180	Slightly corrosive (SC)
180 >	Non-corrosive (NC)

## Results and discussion

The qualitative interpretation of results of the 1-D resistivity (VES) data processed with WinResist software is presented in (Table 3); it defined the lithology and stratigraphic sequence of 5–6 layers. The model curves obtained exhibit thirteen (13) different curve types: KHK taking about 10%, AAKQ, KHAK, KHAA, HKQ, HKQQ and HAA taking 12%, AAA, AKH, HAK and KHKQ taking 24% while AKQ and AAK take 20 and 34%, respectively, which further confirms the variation in lithology, formation and inhomogeneity of the study area. VES profiles were quantitatively analyzed and the results give the geoelectrical information of resistivity, thickness and depth of the subsurface hydro-lithofacies example Fig. 3 which shows the geoelectric curve for VES 7. The first layer resistivity ranged from 40.4 to 3367.1  $\Omega\text{m}$ . This shows that the layer is dominated by low to medium resistive materials made up of sandstone topsoil intercalated with clay. The thickness and depth of this layer varies between 0.5 and 3.9 m. The second geoelectric layer with a resistivity range of 92.2 to 11,730.1  $\Omega\text{m}$  is made of low to high resistivity materials dominated by silty shale to dry unconsolidated sand. This layer is generally less conductive compared to the overlying lithologic units, the thickness and depth of this layer range from 1.5 to 20.4 m and 2.6 to 23.2 m, respectively. The third layer dominated by highly resistivity materials are made of unconsolidated dry sandy silt, this layer on the average is less conductive than the overlying lithologic units. The layer resistivity values ranged from 85.3 to 73,324.3  $\Omega\text{m}$  with thickness and depth ranging from 3.6 to 85.7 and 8.9 to 94.6 m, respectively. The fourth layer has a resistivity range of 153.7 to 91,659.2  $\Omega\text{m}$  with thickness and depth range of 22.4 to 174.3 and 31.3 to 218.4 m. This shows that this layer is also more resistive than the overlying layers; this lithologic unit harbors about 84% of the aquifer in the study area and this agrees with result of Omeje et al. (2021) whose result was obtained from a small part within the study area. The fifth layer has resistivity values ranging from 312.8 to 16,675.1  $\Omega\text{m}$ , the thickness and depth of this layer is undefined except for VES 3, 8, 12, 13, 24, 23 and 38 with ranges of 45.1 to 154.4 and 104.3 to 198.0 m, respectively. This layer is less resistive and more conductive than the overlying layers harboring 14% of

the aquifers in at the study area. The sixth layer is observed only in VES 3, 8, 12, 13, 24, 23 and 38 with resistivity range of 1118.9 to 6892.0  $\Omega\text{m}$  with undefined thickness and depth within the maximum current electrode separations in all the VES stations. It can be said that the sediments in this layer are not compacted, hence lower resistivity values indicating higher conductive geomaterial. Since the layer is below the water table, the sediments in this lithologic unit are considered to be unconsolidated (Mooney, 1980). Generally, it can be inferred from the result that variation in resistivity with depth is majorly affected by geology, topography, drainage system, lithology, water quality and degree of saturation (George et al. 2014).

## Borehole log

The earth materials that dominates the subsurface are fine-medium grain sand, coarse grain sand, dark gray shale, fine grain sand, medium-coarse grain sand, the fine grain sand and the medium-coarse grain sand harbors most of the aquifer layers. The thicknesses of the layers in meters at various depths are evident within the location. The geoelectric layers depth from the VES analysis was constrained using borehole logs obtained from drilling sites close to some VES points as shown in Fig. 4 aided the analysis and interpretation of layers depth and aquifer layers in the study area (Batayneh 2009). The resistivity values from the field survey were constrained using the obtained borehole log to help reduce the intrinsic problems of equivalence and suppression encountered during the interpretation of VES data (George 2021). It also aided the analysis and interpretation by reducing the choice of layer models and identification of the aquifer layer within the locations drilled (Vanovermereen 1989).

Table 4 presents the estimated values of overburden/bulk layer resistivity, conductivity, thickness, GPI, hydraulic conductivity, formation factor, porosity and corrosivity of the first geoelectric layer. The overburden layer resistivity and thickness ranged from 589.8 to 85,094.8  $\Omega\text{m}$  and 8.9 to 99.5 m with mean values of 42,642.3  $\Omega\text{m}$  and 54.2 m. The spread of the overburden resistivity as shown in its contour map (Fig. 5) reveals that low resistivity values dominate the study area indicating presence of high conductive material while the highest overburden resistivity is mainly within the southwestern part. The relatively high resistivity values and the presence of low conducting geomaterials may be attributed to low percolation of subsurface contaminants (Aleke et al. 2018). The aquifer resistivity range obtained in this study area is far higher than the range obtained by Ugwuanyi et al. (2015), Ezema et al. (2020), Obiora and Ibuot (2020), Omeje et al. (2021), who adopted electrical resistivity method to investigate aquifer repositories in little parts of the study area.

**Table 3** Summary of result of resistivity survey form computer modeling using WINRESIST software

S/N	VES points	Longitude ( <sup>o</sup> E)	Latitude ( <sup>o</sup> N)	Resistivity ( $\Omega m$ )			Thickness (m)						Depth (m)					Curve type		
				$\rho_1$	$\rho_2$	$\rho_3$	$\rho_4$	$\rho_5$	$\rho_6$	$h_1$	$h_2$	$h_3$	$h_4$	$h_5$	$d_1$	$d_2$	$d_3$		$d_4$	$d_5$
1	Ibagva-Aka	7.4104	6.9284	437.8	2217.7	15,435.7	8441.0	12,062.4	-	0.9	10.6	49.6	157.3	-	0.9	11.4	61.1	218.4	-	AKH
2	Iheakpu-Awka	7.4228	6.9420	555.5	1372.7	19,509.7	3456.1	5802.1	-	2.7	3.8	36.9	131.3	-	2.7	5.5	42.4	173.7	-	AKH
3	Onicha-Enugu	7.4364	6.9631	327.4	869.7	767.8	12,718.9	11,347.1	6892.0	0.7	3.3	5.0	22.4	154.4	0.7	3.9	8.9	31.3	185.7	KHKQ
4	Ogrute	7.4625	6.9740	277.4	4677.9	9649.0	8456.1	10,748.9	-	1.9	3.8	49.2	81.9	-	1.9	5.6	54.8	136.7	-	AKH
5	Amufie	7.4813	6.9466	488.0	1034.8	36,096.4	45,541.5	8481.8	-	2.9	3.3	19.8	125.6	-	2.9	6.2	26.0	151.6	-	AAK
6	Uda	7.4978	6.9326	317.1	1820.4	30,589.9	30,313.1	3342.9	-	0.9	5.7	33.8	84.4	-	0.9	6.6	29.4	113.8	-	AKQ
7	Obukpa	7.4245	6.8814	143.3	282.3	1379.8	13,527.1	14,013.6	-	3.2	9.4	22.5	123.2	-	3.2	12.6	35.1	158.3	-	AAA
8	Ibeku-Ovoko	7.4373	6.8847	261.9	1138.4	496.1	1467.3	8037.5	4598.6	1.3	6.0	3.6	25.0	76.0	1.3	7.4	11.0	35.9	112.0	KHAK
9	Istija-Ovoko	7.4663	6.8931	200.8	478.6	8104.3	22,417.6	10,843.9	-	3.9	2.8	22.2	153.5	-	3.9	6.6	28.9	182.3	-	AAK
10	Likke—Iheaka	7.4802	6.9003	342.5	748.2	3738.0	12,121.6	10,727.3	-	2.0	9.0	32.7	146.9	-	2.0	11.2	43.9	190.7	-	AAK
11	Obollo-Afor	7.5005	6.9093	355.5	3657.6	8025	23,075.3	8575.8	-	3.1	19.5	22.8	121.0	-	3.1	22.6	45.4	166.4	-	AAK
12	Umuezejor Obollo-Afor	7.5061	6.9257	224.8	1340.1	4496.2	8902.7	8220.0	5027.0	1.6	11.4	34.1	49.9	97.7	1.6	13.0	47.1	97.0	194.8	AAKQ
13	Ugwueghe Obollo-Afor	7.5251	6.9127	300.0	335.2	85.3	153.7	1150.7	6615.1	1.5	9.7	28.5	19.5	45.1	1.5	11.2	39.8	59.2	104.3	KHAA
14	Ogrute II	7.4481	6.9893	464.9	3018.5	790.4	28,708.4	6075.1	-	1.3	4.5	14.7	146.9	-	1.3	5.8	20.5	167.4	-	KHK
15	Imufu	7.4484	7.0030	767.5	306.8	3934.9	9817.9	14,657.1	-	1.5	3.8	50.2	130.3	-	1.5	5.3	55.5	185.8	-	HAA
16	Aji	7.4486	7.0172	979.2	1791.4	7839.8	43,782.5	5663.5	-	1.5	10.9	12.2	89.4	-	1.5	12.4	24.6	114.0	-	AAK
17	Aji II	7.4490	7.0369	893.2	1291.1	1030.6	9963.8	2808.5	-	3.3	9.6	25.3	158.4	-	3.3	12.9	38.1	196.5	-	KHK
18	Umuodeje	7.4478	7.0656	494.3	1352.3	1558.4	5858.5	9518.4	-	2.1	13.1	26.0	169.2	-	2.1	15.2	41.1	210.3	-	AAA
19	Umuadogwu	7.4372	6.9837	62.0	512.3	13,449.4	91,659.2	16,675.1	-	2.5	1.5	9.9	174.3	-	2.5	3.9	13.8	188.1	-	AAK
20	Inere	7.4176	6.9857	1170.9	346.5	3936.2	17,220.0	4678.2	-	1.1	4.8	32.2	137.1	-	1.1	5.9	38.1	175.2	-	HAK
21	Alor-Uno I	7.3866	6.8716	386.5	1175.2	2653.7	4612.0	2915.6	-	3.8	4.2	42.1	157.9	-	3.8	8.0	50.0	207.9	-	AAK
22	Anwama—Amufie	7.4689	6.9457	247.6	2811.8	2801.3	28,296.2	10,195.4	-	0.6	14.7	24.7	172.6	-	0.6	15.4	40.1	212.8	-	KHK
23	Lejja	7.3908	6.8057	3367.1	1625.6	35,090.5	27,910.8	8149.1	4768.6	2.7	5.7	30.7	60.4	111.7	2.7	8.4	39.1	99.4	211.1	HKQQ
24	Igogoro I	7.4703	6.9897	335.4	1383.8	1013.3	11,094.0	2388.8	1118.9	1.5	9.0	18.1	69.7	99.7	1.5	10.4	28.6	98.3	198.0	KHKQ
25	Igogoro II	7.4835	6.9951	662.3	6909.8	27,910.4	11,783.9	712.8	-	1.2	18.7	50.9	55.2	-	1.2	19.9	70.8	126.0	-	AKQ
26	Uroshi	7.4760	6.9617	127.1	92.2	8241.6	5421.4	514.2	-	2.0	3.7	23.4	75.0	-	2.0	5.7	29.1	104.1	-	HKQ
27	IGbelle	7.4841	6.9698	131.8	430.3	4617.3	15,647.1	4502.2	-	0.8	10.8	16.2	158.4	-	0.8	11.6	27.8	186.2	-	AAK
28	Istobere	7.4804	6.9567	873.3	3310.2	31,371.0	6169.3	1062.8	-	1.3	12.2	49.6	55.6	-	1.3	13.6	63.1	118.7	-	AKQ
29	Amufie II	7.4640	6.9483	200.7	2637.5	5470.4	19,095.0	470.0	-	1.1	13.4	14.1	57.5	-	1.1	14.5	28.6	86.1	-	AAK
30	ISIenu Nsukka	7.4392	6.8420	105.9	508.6	39,497.9	9095.5	6457.5	-	0.7	4.7	46.1	136.4	-	0.7	5.4	51.5	187.9	-	AKQ
31	AGbamere Eha- Alumona	7.4546	6.8275	1193.7	300.2	13,791.4	58,535.7	7879.2	-	2.8	5.2	10.9	133.0	-	2.8	8.0	18.9	152.0	-	HAK
32	Umuabo Eha-Alumona I	7.4523	6.8203	357.3	717.1	1850.5	5072.8	7960.6	-	2.4	5.1	74.8	111.9	-	2.4	7.5	82.3	194.2	-	AAA
33	Eha—Alumona	7.4543	6.8161	857.7	1822.2	17,967.0	2762.6	312.8	-	2.2	12.6	42.8	56.3	-	2.2	14.7	57.5	113.8	-	AKQ
34	Umuabo Eha—Alumona II	7.4500	6.8104	836.6	1665.9	3542.2	6835.1	663.6	-	2.5	7.7	31.6	94.0	-	2.5	10.3	41.9	135.9	-	AAK
35	Ede-Oballa	7.4286	6.8010	60.3	1141.6	1106.2	8270.7	3208.2	-	0.6	20.4	23.3	133.7	-	0.6	20.9	44.2	178.0	-	KHK
36	Ama—Ezike	7.4194	6.8036	40.4	11,730.1	73,324.3	3473.0	1328.5	-	0.5	2.1	30.4	85.8	-	0.5	2.6	33.1	118.9	-	AKQ

Table 3 (continued)

S/N	VES points	Longitude (°E)	Latitude (°N)	Resistivity ( $\Omega m$ )						Thickness (m)					Depth (m)					Curve type
				$\rho_1$	$\rho_2$	$\rho_3$	$\rho_4$	$\rho_5$	$\rho_6$	$h_1$	$h_2$	$h_3$	$h_4$	$h_5$	$d_1$	$d_2$	$d_3$	$d_4$	$d_5$	
37	Edem Rd	7.3759	6.8652	1332.7	2929.6	6965.9	34,765.9	1008.8	-	0.7	16.8	13.8	62.2	-	0.7	17.5	31.3	93.5	-	AAK
38	Ogobdu Nsukka	7.3689	6.8717	2902.1	4592.9	2266.3	32,864.0	5423.4	1258.5	1.2	6.1	15.0	55.3	66.7	1.2	7.2	22.2	77.5	144.2	KHKQ
39	Imirikii Ogbogidi	7.3604	6.8781	173.1	285.6	2550.4	31,370.7	3496.2	-	1.4	15.4	11.7	155.0	-	1.4	16.8	28.5	183.5	-	AAK
40	Tech College Amogwu	7.3543	6.8543	1841.1	3364.5	3089.5	17,309.2	957.3	-	1.1	9.9	23.9	84.6	-	1.1	11.0	34.9	199.6	-	KHK
41	Army Barracks Nsukka	7.3649	6.8515	1614.6	3511.8	16,591.8	9534.3	954.7	-	3.0	20.2	55.8	67.4	-	3.0	23.2	79.1	146.5	-	AKQ
42	Alor-Uno II	7.3837	6.8692	341.5	1149.6	3364.3	17,419.6	442.0	-	0.8	17.9	13.1	61.5	-	0.8	18.7	31.8	93.2	-	AAK
43	Secretariat Ibagwa-Aka	7.4005	6.9243	99.0	243.2	444.5	2,349.2	484.4	-	1.1	16.0	17.4	96.1	-	1.1	17.1	34.5	130.5	-	AAK
44	Alor-Uno III	7.3714	6.8877	216.2	108.8	264.8	2981.2	1710.3	-	0.8	3.6	36.3	157.8	-	0.8	4.4	40.7	198.5	-	HAK
45	Eburummiri Ibagwa-Aka	7.3950	6.9362	3092.7	4081.8	8275.5	16,867.4	239.0	-	3.9	19.0	25.3	51.0	-	3.9	22.9	48.2	99.2	-	AAK
46	Uzoogo Ibagwa-Aka	7.4032	6.9303	435.9	833.1	12,652.6	4091.6	317.8	-	1.2	7.7	85.7	50.1	-	1.2	8.9	94.6	144.6	-	AKQ
47	Ngwo Ibagwa-Aka	7.3849	6.9360	203.9	1985.4	9431.1	1579.3	1169.0	-	1.3	2.1	23.9	158.7	-	1.3	3.4	27.3	186.0	-	AKQ
48	Ikem Ibagwa-Aka	7.3956	6.9296	204.7	893.3	11,550.7	2088.7	408.6	-	1.0	14.6	50.5	53.6	-	1.0	15.6	66.1	119.7	-	AKQ
49	Itchi	7.3647	6.9552	878.9	1016.1	1756.1	17,516.9	427.5	-	1.9	12.6	11.1	51.9	-	1.9	14.6	25.7	77.6	-	AAK
50	Itchi Obukpa	7.3647	6.9553	632.5	1349.2	9649.6	12,525.7	738.5	-	1.0	17.5	21.7	65.8	-	1.0	18.4	40.1	105.8	-	AAK

The contour map of the overburden thickness (Fig. 6) shows the variation of this parameter across the area depicting areas with high to low thickness of geologic material. It is shown that areas with high overburden resistivity correspond to areas with high overburden thickness and vice versa. The aquifer units located in areas with high overburden thickness may likely have high protective capacity and may not be vulnerable to pollution (Burger et al. 1992; Obiora and Ibuot 2020). Results of aquifer thickness corresponds with the results of aquifer thickness determined by Ugwuanyi et al. (2015), Ezema et al. (2020), Obiora and Ibuot (2020) and Omeje et al. (2021) who studied aquifer characteristics in areas having similar geologic features with some part of the study area showing similar trend variation with aquifer thickness of this study area though of different magnitude. This shows that areas with similar geologic features can vary in groundwater accumulation.

The estimated GPI of the overlying layer has value ranging from 0.0004 to 0.0690  $\Omega^{-1}$  with average value of 0.0010  $\Omega^{-1}$  while the hydraulic conductivity ( $K$ ) of the overlying layer has values varying from 0.0097 to 1.0056 mday<sup>-1</sup> with average value of 0.5077 mday<sup>-1</sup>. The GPI contour map in Fig. 7 revealed areas with high and low vulnerability and its rating in Table 4 using Table 1 is from weak to fair level of contamination. Some areas in the western and eastern part of the study area have aquifers with the highest risk of contamination. Since the earth medium act as a natural filter to the percolating fluid, its ability to retard fluid infiltrating into the subsurface is a measure of its protective capacity (Mogaji et al. 2007; Obiora et al., 2015; Obiora and Ibuot 2020; Ossai et al., 2020). This implies that aquifers in the areas with low protection level have the highest tendency to being protected from polluted leachates easily due to high overburden resistivity and thickness with low porosity and hydraulic conductivity of the overlying layer (Mallums et al. 2019). This result of GPI is consistent with that of Ossai et al. (2020) who employed aquifer vulnerability index (AVI) method in carrying out vulnerability assessment.

The spread of hydraulic conductivity (Fig. 8) for the overburden layers reveal that the western and eastern part of the study area have the highest value of overburden hydraulic conductivity implying high infiltration and good area for groundwater accumulation. The hydraulic conductivity ranged from 0.009 to 0.539  $\Omega^{-1} m^{-1}$  with an average of 0.274  $\Omega^{-1} m^{-1}$ . It is observed that areas with maximum value of GPI correspond to areas of high hydraulic conductivity and porosity, indicating that the zone is being saturated with contaminants of high conductive minerals in the aquifer layers. The Southwestern and part of Southeastern in the study area is observed to have high hydraulic conductivity values while low values trend from the North to South. The high value is an indication of high conductivity, high



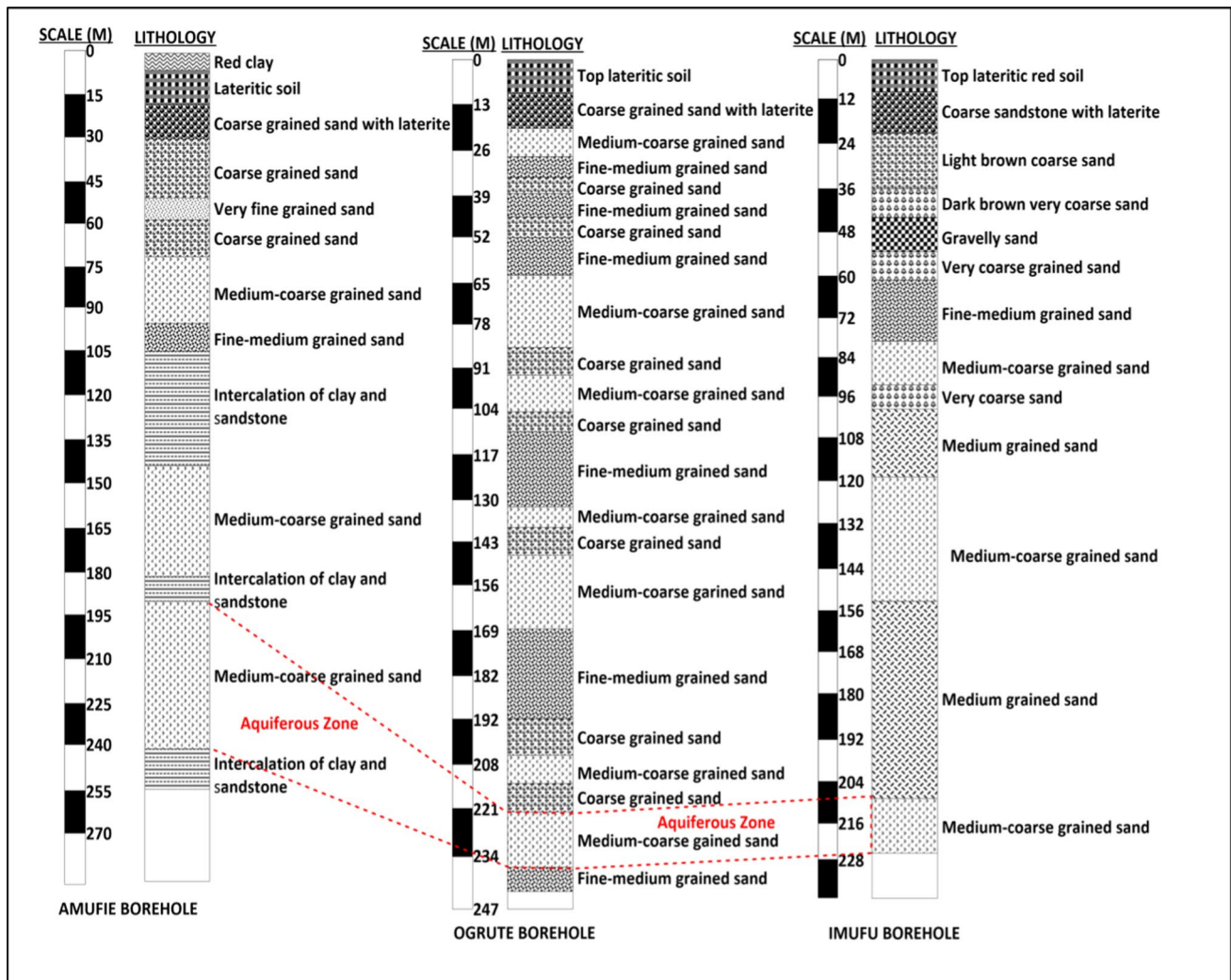


**Fig. 4** Borehole lithology logs. a: borehole lithologic log close to VES 5, 22 and 29, b: borehole lithologic log close to VES 4, c: borehole lithologic log close to VES 15

porosity, high transmissivity, low resistivity and low thickness (Oseji et al. 2018).

The fractional porosity value of the overlaying layers ranged from 4.6553 to 25.5253 with the mean values of 15.0903 while the value of the formation factor ( $F$ ) ranged from 0.0039 to 0.0498 with the mean value of 0.0268. It can be inferred that the porosity of the overlaying layer influences the easy flow of fluid during infiltration, low to moderate porosity level sweeps across the area except some part in the western and eastern region which has high bulk porosity level in Fig. 9 corresponding to high bulk hydraulic conductivity. This implies that a highly porous layer allows free flow of fluids. On the contrary, areas of high formation factor correspond to area of high bulk thickness and resistivity as shown in the contour map (Fig. 10), areas with high porosity is attributed to areas with low formation factor and vice versa. When the formation factor is high, the hydraulic

conductivity, porosity, recharge and infiltration rate will be very low. The variation of elevation in the study area considered as one of the factors influencing groundwater movement and transmission and zones with low elevation are associated with low overburden thickness and resistivity, high GPI, high risk of contamination, high porosity, hydraulic conductivity and vice versa.

Corrosivity describes how aggressive water is at destroying or weakening (corroding) pipes and equipment. Corrosive water reduces the quality of groundwater and can lead to health related problems such high blood pressure, gastro intestine disease and kidney and liver problems. Corrosivity of soil in the study area was determined using the first layer resistivity and comparing with that of Table 2. The first layer soil of all the VES locations has resistivity value greater than 180  $\Omega$ m indicating that the soil materials are practically non-corrosive agrees with results of Roberge 2000, Omeje et al.

**Table 4** Calculated GPI and overburden geohydraulic parameters from resistivity and thickness of overlying layers

VES S/N	VES stations	Longitude (°E)	Latitude (°N)	Bulk resist $\rho$ ( $\Omega\text{m}$ )	Bulk conduct ( $\Omega\text{m}^{-1}$ )	Bulk thickness $h$ (m)	Bulk K (m/day)	Bulk porosity ( $\phi$ )	Bulk formation factor	GPI ( $\Omega^{-1}$ )	GPI rating	First layer resist. ( $\Omega\text{m}$ )	Corrosivity
1	Ibagwa-Aka	7.4104	6.9284	18,091.2	5.53E-05	61.1	0.083	14.274	0.009	0.003	WEAK	437.8	NC
2	Iheakpu-Awka	7.4228	6.9420	21,437.9	4.66E-05	42.4	0.035	10.442	0.015	0.002	WEAK	555.5	NC
3	Onicha-Enugu	7.4364	6.9631	14,683.8	6.81E-05	31.4	0.050	12.031	0.020	0.002	WEAK	327.4	NC
4	Ogrute I	7.4625	6.9740	14,604.3	6.85E-05	54.9	0.050	12.054	0.012	0.004	WEAK	277.4	NC
5	Amufie I	7.4813	6.9466	37,619.2	2.66E-05	26	0.021	8.082	0.022	0.001	WEAK	488.0	NC
6	Uda	7.4978	6.9326	32,727.4	3.06E-05	29.4	0.024	8.666	0.020	0.001	WEAK	317.1	NC
7	Obukpa	7.4245	6.8814	1805.5	0.000554	35.1	0.354	20.829	0.005	0.019	WEAK	143.3	SC
8	Ibeku Ovoko	7.4373	6.8847	3363.7	0.000297	35.9	0.198	18.217	0.006	0.011	WEAK	261.9	NC
9	Isiuja Ovoko	7.4663	6.8931	8783.7	0.000114	28.9	0.081	14.188	0.009	0.003	WEAK	200.8	NC
10	Iheaka	7.4802	6.9003	4828.7	0.000207	43.9	0.142	16.699	0.007	0.009	WEAK	342.5	NC
11	Obollo-Afor	7.5005	6.9093	12,038.7	8.31E-05	45.4	0.060	12.865	0.011	0.004	WEAK	355.5	NC
12	Umuezejor Obollo-Afor	7.5061	6.9257	14,963.7	6.68E-05	97	0.050	11.952	0.012	0.007	WEAK	224.8	NC
13	Ugwuegbe Obollo-Afor	7.5251	6.9127	874.2	0.001144	59.2	0.697	23.873	0.004	0.068	FAIR	300.0	NC
14	Ogrute II	7.4481	6.9893	4273.0	0.000234	20.5	0.159	17.213	0.007	0.005	WEAK	464.9	NC
15	Imufu	7.4484	7.0030	5009.2	0.0002	55.5	0.137	16.545	0.007	0.011	WEAK	767.5	NC
16	Aji I	7.4486	7.0172	10,610.4	9.42E-05	24.6	0.068	13.395	0.010	0.002	WEAK	979.2	NC
17	Aji II	7.4490	7.0369	3214.9	0.000311	38.2	0.207	18.407	0.006	0.012	WEAK	893.2	NC
18	Umuodeje	7.4478	7.0656	3405	0.000294	41.2	0.196	18.166	0.007	0.012	WEAK	494.3	NC
19	UmuAdogwu	7.4372	6.9837	14,023.7	7.13E-05	13.9	0.052	12.224	0.012	0.001	WEAK	62.0	SC
20	Inere	7.4176	6.9857	5453.6	0.000183	38.1	0.126	16.189	0.008	0.007	WEAK	1170.9	NC
21	Alor- Uno I	7.3866	6.8716	4215.4	0.000237	50.1	0.161	17.270	0.008	0.012	WEAK	386.5	NC
22	Anwama Amufie	7.4689	6.9457	5860.7	0.000171	40	0.118	15.886	0.008	0.007	WEAK	247.6	NC
23	Lejja	7.3908	6.8057	67,994	1.47E-05	99.5	0.012	5.597	0.038	0.002	WEAK	3367.1	NC
24	Igogoro I	7.4703	6.9897	13,826.5	7.23E-05	98.3	0.053	12.283	0.012	0.007	WEAK	335.4	NC
25	Igogoro II	7.4835	6.9951	34,681.5	2.88E-05	70.8	0.022	8.423	0.021	0.002	WEAK	662.3	NC
26	Uroshi	7.476	6.9617	8460.9	0.000118	29.1	0.084	14.345	0.009	0.003	WEAK	127.1	SC
27	IGbelle	7.4841	6.9698	5179.4	0.000193	27.8	0.133	16.405	0.008	0.005	WEAK	131.8	SC
28	Isiobere	7.4804	6.9567	35,554.5	2.81E-05	63.1	0.022	8.319	0.021	0.002	WEAK	873.3	NC
29	Amufie II	7.4640	6.9483	8308.6	0.00012	28.6	0.085	14.421	0.009	0.003	WEAK	200.7	NC
30	ISienu Nsukka	7.4392	6.8420	40,112.4	2.49E-05	51.5	0.020	7.812	0.023	0.001	WEAK	105.9	SC
31	AGbamere Eha-Alumona	7.4546	6.8275	15,285.3	6.54E-05	18.9	0.048	11.862	0.012	0.001	WEAK	1193.7	NC
32	Umuabo EhaAlumona	7.4523	6.8203	2924.9	0.000342	82.3	0.226	18.804	0.006	0.028	WEAK	357.3	NC

Table 4 (continued)

VES S/N	VES stations	Longitude (°E)	Latitude (°N)	Bulk resist $\rho$ ( $\Omega\text{m}$ )	Bulk conduct ( $\Omega\text{m}^{-1}$ )	Bulk thickness $h$ (m)	Bulk K (m/day)	Bulk porosity ( $\phi$ )	Bulk formation factor	GPI ( $\Omega^{-1}$ )	GPI rating	First layer resist. ( $\Omega\text{m}$ )	Corrosivity
33	Eha- Alumona	7.4543	6.8161	20,646.9	4.84E-05	57.6	0.036	10.600	0.015	0.003	WEAK	857.7	NC
34	Umuabor Ehaalumoa II	7.4500	6.8104	6044.7	0.000165	41.8	0.115	15.757	0.008	0.007	WEAK	836.6	NC
35	Ede Oballa	7.4286	6.8010	2308.1	0.000433	44.3	0.282	19.798	0.006	0.019	WEAK	60.3	SC
36	Ama- Ezike	7.4194	6.8036	85,094.8	1.18E-05	33	0.010	4.655	0.050	0.000	WEAK	40.4	MC
37	Edem Rd	7.3759	6.8652	11,228.2	8.91E-05	31.3	0.064	13.157	0.011	0.003	WEAK	1332.7	NC
38	Ogbodu	7.3689	6.8717	42,625.3	2.35E-05	77.6	0.019	7.557	0.024	0.002	WEAK	2902.1	NC
39	Imirikin Ogbogidi	7.3604	6.8781	3009.1	0.000332	28.5	0.220	18.685	0.006	0.010	WEAK	173.1	SC
40	Tech-College Amogwu	7.3543	6.8543	8295.1	0.000121	34.9	0.085	14.428	0.009	0.004	WEAK	1841.1	NC
41	Army-Barracks Nsukka	7.3649	6.8515	21,718.2	4.6E-05	79.0	0.035	10.388	0.015	0.004	WEAK	1614.6	NC
42	Alor Uno II	7.3837	6.8692	4855.4	0.000206	31.8	0.141	16.676	0.007	0.007	WEAK	341.5	NC
43	Alor Uno III	7.4005	6.9243	589.8	0.001695	40.7	1.006	25.525	0.004	0.069	FAIR	99.0	SC
44	Secretariat Ibagwa- Aka	7.3714	6.8877	786.7	0.001271	34.5	0.769	24.316	0.004	0.044	WEAK	216.2	NC
45	Eburummiri Ibagwa-Aka	7.3950	6.9362	15,450	6.47E-05	48.2	0.048	11.817	0.012	0.003	WEAK	3092.7	NC
46	Uzoego IbagwaAka	7.4032	6.9303	8769	0.000114	8.9	0.081	14.195	0.009	0.001	WEAK	435.9	NC
47	Ngwo Ibagwa Aka	7.3849	6.9360	11,620.4	8.61E-05	27.3	0.062	13.013	0.011	0.002	WEAK	203.9	NC
48	Ikem Ibagwa-Aka	7.3956	6.9296	12,648.7	7.91E-05	66.1	0.058	12.657	0.011	0.005	WEAK	204.7	NC
49	Itchi	7.3647	6.9552	3651.1	0.000274	25.6	0.184	17.873	0.007	0.007	WEAK	878.9	NC
50	Itchi Obukpa	7.3647	6.9553	11,631.3	8.6E-05	40.2	0.062	13.009	0.011	0.004	WEAK	632.5	NC

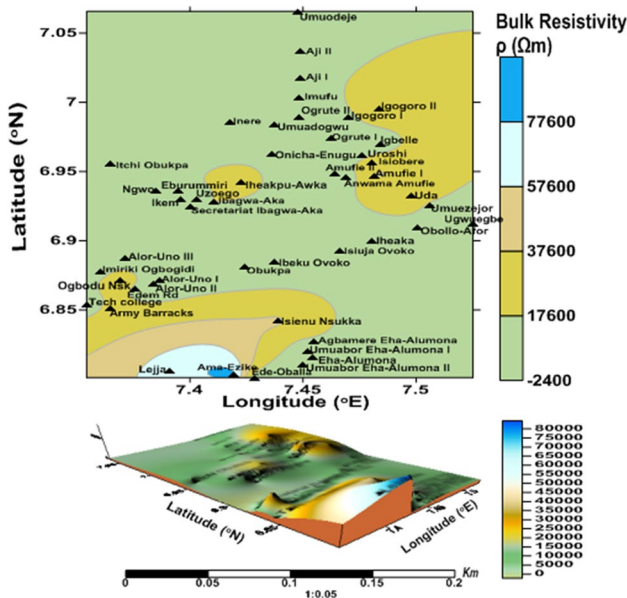


Fig. 5 2D and 3D contour map showing the variation of bulk resistivity in the study area

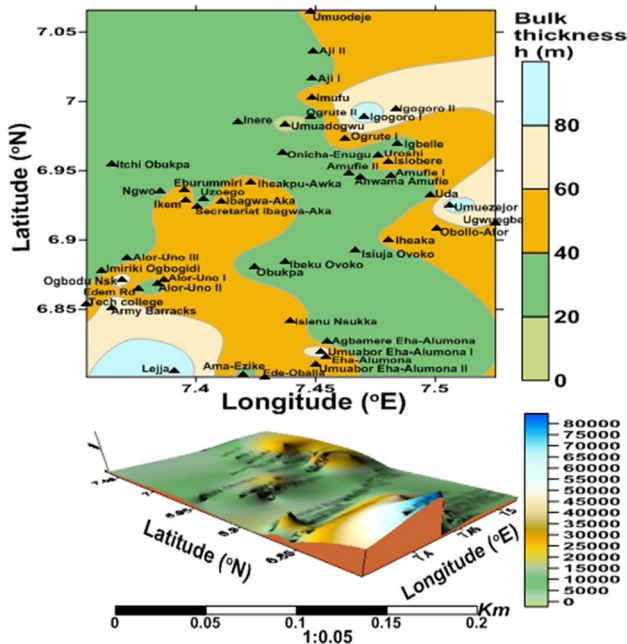


Fig. 6 2D and 3D contour map showing the variation of bulk thickness in the study area

(2021) and can favor the laying/burying of underground iron tanks/pipes without deterioration or rusting. VES 19, 35 and 43 have resistivity of the soil materials less than 180 Ωm but greater than 60 Ωm, this is an indication of slightly corrosive geomaterials which when in contact with metals pipes can

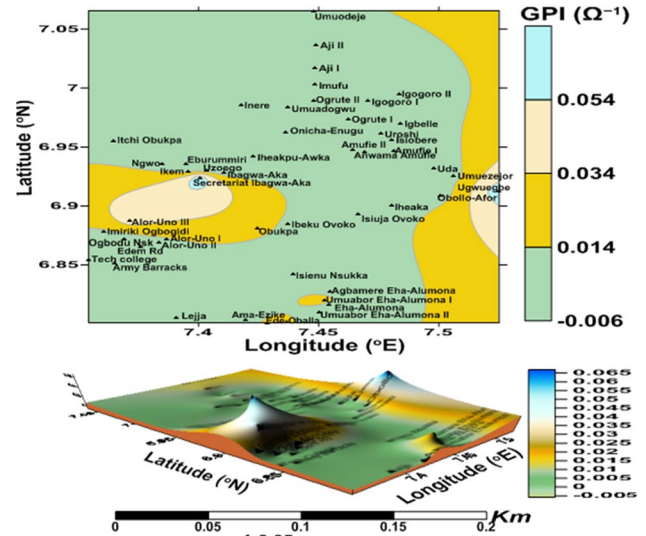


Fig. 7 2D and 3D contour map showing the variation of GPI in the study area

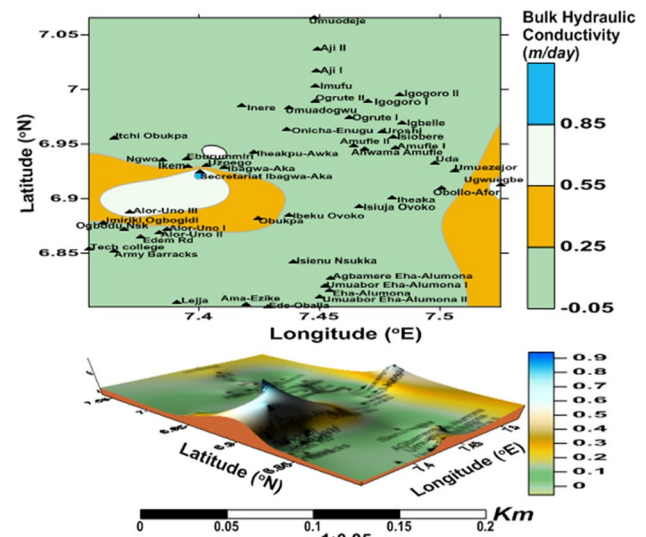
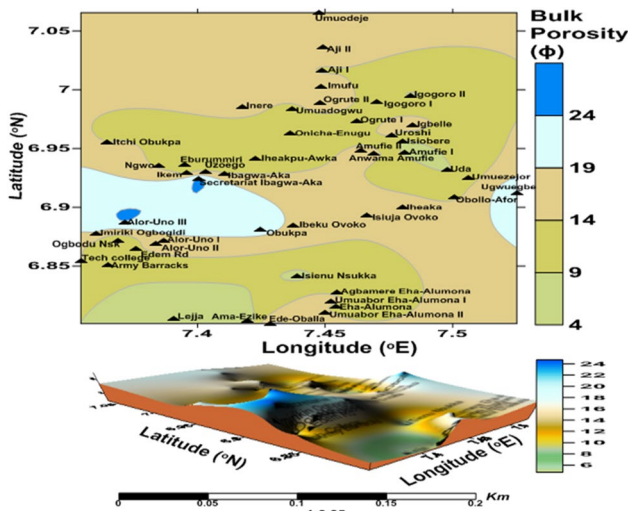


Fig. 8 2D and 3D contour map showing the variation of bulk hydraulic conductivity in the study area

corrode the pipes, hence not suitable for laying underground pipes but concrete and steel underground reservoirs can be constructed for water storage. This result and suggestions compares positively with the works of Obiora et al., 2016. The second layer is practically non-corrosive and is hereby advised that engineers should go beyond the first layer while installing metal pipes beneath the earth surface in those locations whose geomaterials can be slightly or moderately corrosive or install plastic pipes.



**Fig. 9** 2D and 3D contour map showing the variation of bulk porosity in the study area

### Conclusion

Electrical resistivity method was successfully employed to evaluate the groundwater repositories in terms of groundwater potential and protective capacity of parts of Enugu North, Eastern Nigeria. The results of the geoelectric survey revealed that the study area is made up of five to six geoelectric layers and different geoelectric curves obtained revealed the heterogeneity and variation in lithologic formation within the study area. The fourth and fifth layers were found to harbor most of the aquifer units with some parts having low groundwater potential. Some areas in the western and eastern part of the study area have high risk of groundwater protection against contamination while other locations with low protection level are not vulnerable to contamination from surface contaminants. It is inferred from the study that hydraulic conductivity and porosity in the Southwest is high indicating that the groundwater potential will be good in VES 47 and its environ though with high risk of being contaminated. A good borehole in the study area should be drilled to a depth within the fourth and fifth layer (aquifer unit). Most of VES points in the first layer are practically non-corrosive which implies that the top layer is made up of geologic materials that cannot cause corrosion of pipes or any metal. This study have thrown more light in the understanding of the aquifer protective capacity, corrosive nature, groundwater potential and the properties of the aquifer repositories in the inhomogeneous study area which will serve as a guide to other researchers and borehole drillers for effective groundwater development, management and exploiting aquifers with good protective capacity in order to obtain potable water. Based on the results from this research

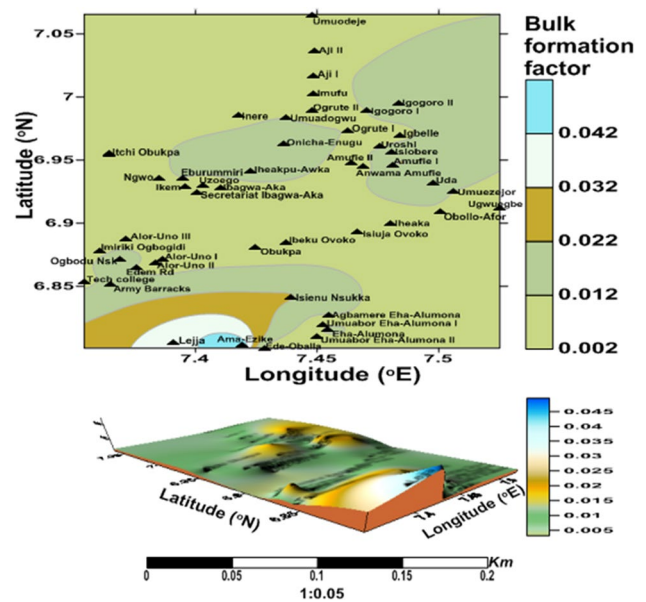


**Fig. 10** 2D and 3D contour map showing the variation of bulk formation factor in the study area

it is suggested that aquifer in areas that have low or little contamination risk should be explored while attempt should be made in those areas with high pollution risk to reduce the pollution rate by total stoppage of refuse dumping, laying sewage pipes and treatment of pumping water before use. Finally this study showcased that GPI is an important method in delineating hydrogeological units that are prone to contamination by virtue of the unique combined effect of the overlying layer thicknesses. Since adequately thick aquifer overlying layer could prolong/delay the transit time of contaminants into aquifers underneath thereby degrading the contaminants caused by the synergistic effects of geologic and biogenic activities and making such areas not to be minimally weak to pollution. Areas with high GPI values are associated with low values of overburden thickness which makes the protective capacity to be weak and susceptible to pollution.

**Funding** The authors did not receive funds, grants or support from any organization for the submitted work.

### Declarations

**Conflict of interest** The authors have no conflicts of interest that are relevant to the content of this manuscript.

**Ethical approval** This manuscript is original and not submitted to any other journal for consideration.

**Human or animal rights** This research does not involve human or animal participants.

**Open Access** This article is licensed under a Creative Commons Attribution 4.0 International License, which permits use, sharing, adaptation, distribution and reproduction in any medium or format, as long as you give appropriate credit to the original author(s) and the source, provide a link to the Creative Commons licence, and indicate if changes were made. The images or other third party material in this article are included in the article's Creative Commons licence, unless indicated otherwise in a credit line to the material. If material is not included in the article's Creative Commons licence and your intended use is not permitted by statutory regulation or exceeds the permitted use, you will need to obtain permission directly from the copyright holder. To view a copy of this licence, visit <http://creativecommons.org/licenses/by/4.0/>.

## References

- Abdalla CW (1990) Measuring economic losses from ground water contamination: an investigation of household avoidance costs. *Water Resour Bull* 26(3):451–463
- Agunlope O (1984) Soil aggressivity along steel pipeline route at Ajakuta southwestern Nigeria. *J Min Geol* 21:97–101
- Aleke CG, Ibuot JC, Obiora DN (2018) Application of electrical resistivity method in estimating geohydraulic properties of a sandy hydrolithofacies: a case study of Ajali Sandstone in Ninth Mile, Enugu State, Nigeria. *Arab J Geosci* 11:322. <https://doi.org/10.1007/s12517-018-3638-8>
- Baeckmann WV, Schwenk W (1975) Handbook of cathodic protection: the theory and practice of electrochemical corrosion protection technique. Cambridge Press
- Black RE, Morris S, Bryce J (2003) Where and why are 10 million children dying every year? *Lancet* 361(9376):2226–2234
- Burger HR (1992) Exploration geophysics of shallow subsurface practice. Prentice Hall
- Casas A, Himi M, Diaz Y et al (2008) Assessing aquifer vulnerability to pollutants by electrical resistivity tomography (ERT) at a nitrate vulnerable zone in NE Spain. *Environ Geol* 54:515–520
- Duan W, Kaoru T (2020) Impacts of climate and human activities on water resources and quality. Springer, Amsterdam
- Ekanem AM (2020) Georesistivity modelling and appraisal of soil water retention capacity in Akwa Ibom State University main campus and its environs Southern Nigeria. *Model Earth Syst Environ* 6(4):2597–2608. <https://doi.org/10.1007/s40808-020-00850-6>
- Ezeh CC, Ugwu GZ (2010) Geoelectrical sounding for estimating groundwater potential in Nsukka L.G.A. Enugu State, Nigeria. *Int J Phys Sci* 5(5):415–420
- Ezeh CC (2012) Hydrogeophysical studies for the delineation of potential groundwater zones in Enugu State, Nigeria. *Int Res J Geol Min (IRJGM)* 2(5):103–112
- Ezema OK, Ibuot JC, Obiora DN (2020) Geophysical investigation of aquifer repositories in Ibagwa Aka, Enugu State, Nigeria, using electrical resistivity method. *Groundw Sustain Dev*. <https://doi.org/10.1016/j.gsd.2020.100458>
- Ganiyu SA, Badmus BS, Oladunjoye MA et al (2015) Delineation of leachate plume migration using electrical resistivity imaging on lapite dumpsite in Ibadan Southwestern Nigeria. *Geosciences* 5(2):70–80
- George NJ, Akpan AO, Umoh A (2013) Preliminary geophysical investigation to delineate the groundwater conductive zones in the coastal region of Akwa Ibom State, Southern Nigeria, around the Gulf of Guinea. *Int J Geosci* 4(1):108–115
- George NJ, Nathaniel EU, Etuk SE (2014) Assessment of economically accessible groundwater reserve and its protective capacity in eastern Obolo local government area of Akwa Ibom State, Nigeria using electrical resistivity method. Hindawi Publishing Corporation ISRN Geophysics
- George JN, Ibuot JC, Obiora DN (2015) Geoelectrohydraulic parameters of shallow sandy aquifer in Itu, Akwa Ibom State (Nigeria) using geoelectric and hydrogeological measurements. *J Afr Earth Sci* 110:52–63
- George NJ, Atat JG, Umoren EB et al (2017) Geophysical exploration to estimate the surface conductivity of residual argillaceous bands in the groundwater repositories of coastal sediments of Eolga, Nigeria. *NRIAG J Astron Geophys*. <https://doi.org/10.1016/j.nrjag.2017.02.001>
- Heigold PC, Gilkeson RH, Cartwright K et al (1979) Aquifer transmissivity from surficial electrical methods. *Groundwater* 17(4):338–345
- Ibuot JC, Akpabio GT, George NJ (2013) A survey of the repositories of groundwater potential and distribution using geoelectrical resistivity method in Itu Local Government Area (L.G.A), Akwa Ibom State Southern Nigeria. *Cent Eur J Geosci* 5(4):538–547
- Ibuot JC, Obiora DN, Ekpa MM et al (2017a) Geoelectrohydraulic investigation of the surficial aquifer units and corrosivity in parts of Uyo L. G. A., Akwa Ibom, Southern Nigeria. *J Appl Water Sci* 7:4705–4713
- Ibuot JC, Okeke FN, George NJ et al (2017b) Geophysical and physicochemical characterization of organic waste contamination of hydrolithofacies in the coastal dumpsite of Akwa Ibom State, Southern Nigeria. *Water Sci Technol Water Supply* 17(6):1626–1637
- Ibuot JC, Okeke FN, Obiora DN et al (2019a) Assessment of impact leachate on hydrogeological repositories in Uyo, Southern Nigeria. *J Environ Eng Sci* 14(2):97–107
- Ibuot JC, George NJ, Okwesili NA et al (2019b) Investigation of lithotextural characteristics of aquifer in Nkanu West Local Government Area of Enugu state, southeastern Nigeria. *J Afr Earth Sci* 153:197–207
- Ibuot JC, Ekpa MM, Okoroh DO et al (2020) Geoelectric study of groundwater repository in parts of Akwa Ibom State, Southern Nigeria. *Water Conserv Manag* 4(2):99–102
- Ibuot JC, Obiora DN (2021) Estimating geohydrodynamic parameters and their implications on aquifer repositories: a case study of University of Nigeria, Nsukka Enugu State. *Water Pract Technol* 16(1):162–181
- Keary P, Brooks M (1991) An introduction to geophysical exploration, 2nd edn. Blackwell Scientific Publications, London
- Loke MH (2001) Electrical imaging surveys for environmental and engineering studies. A practical guide to 2D and 3D surveys. Res2Dinv manual. IRIS instruments. [www.iris.instruments.com](http://www.iris.instruments.com)
- Macdonald AM, Robins NS, Ball DF, O Dochartaigh BE (2005) An overview of groundwater development in Scotland. *Scott J Geol* 41(1):3–11
- Maillet R (1947) The fundamental equations of electrical prospecting. *Geophysics* 12:529–556
- Mallums MS, Abubakar IY (2019) Evaluation of groundwater potential and aquifer characteristics using geoelectrical method In Billiri And Environs part of sheet 173 Kaltungo Nw Northern Eastern Nigeria. *Savanna* 1(1):41–45
- Marotz G (1968) TechnischeGrundlageneinerwasserspeicherungim-naturlichenuntergrund. Verlag Wasser Und Boden, Hamburg
- Mogaji KA, Adiat KAN, Oladapo MI (2007) Geoelectric investigation of the Dape Phase IIIhousing Estate, FCT Abuja, North central Nigeria. *J Earth Sci* 1(2):76–84
- Mooney HM (1980) Handbook of engineering geophysics: vol 2, electrical resistivity: Minneapolis, Minnesota. Bison instruments
- Obiora DN, Ajala AE, Ibuot JC (2015) Evaluation of aquifer protective capacity of overburden unit and soil corrosivity in Makurdi, Benue state, Nigeria, using electrical resistivity method. *J Earth Syst Sci* 124(1):125–135

- Obiora DN, Alhassan UD, Ibuot JC et al (2016) Geoelectric evaluation of aquifer potential and vulnerability of Northern Paiko, Niger State, Nigeria. *Water Environ Res* 88(7):644–651
- Obiora DN, Ibuot JC (2020) Geophysical assessment of aquifer vulnerability and management: a case study of University of Nigeria, Nsukka, Enugu State. *Appl Water Sci* 10(1):1–11
- Ochuko A, Oseme JI, Iserhien-Emekeme RE et al (2021) Determination of groundwater potential and aquifer hydraulic characteristics in Agbor, Nigeria using geo-electric, geophysical well logging and pumping test techniques. *Model Earth Syst Environ* 7(1):1639–1649
- Oladapo MI, Mohammed MZ, Adeoye OO et al (2004) Geoelectric investigation of the Ondo State Housing Corporation Estate; Ijapo, Akure, southwestern Nigeria. *J Min Geol* 40(1):41–48
- Omeje ET, Ugbor DO, Ibuot JC et al (2021) Assessment of groundwater repositories in Edem, Southeastern Nigeria, using vertical electrical sounding. *Arab J Geosci* 14(421):1–10
- Omogunloye OG, Jimoh RA (2013) Assessment of groundwater pollution using geophysical norms and GIS as a tool: a case study of part of Ikeja, Lagos State, Nigeria, West Africa. *Glob J Hum Soc Sci Geogr Geo-Sci Environ Disaster Manag* 13(8):1–10
- Oseji JO, Egbai JC, Okolie EC et al (2018) Investigation of the aquifer protective capacity and groundwater quality around some open dumpsites in Sapele Delta State Nigeria. *Appl Environ Soil Sci* 2018:1–18
- Ossai MN, Okeke FN, Obiora DN et al (2020) Vulnerability assessment of hydrogeologic units in parts of Enugu North, Southeastern Nigeria, using integrated electrical resistivity methods. *Indian J Sci Technol* 13(34):3495–3509
- Pomposiello C, Dapena C, Favetto A et al (2012) Application of geophysical methods to waste disposal studies, municipal and industrial waste disposal. In: Yu X-Y (ed) *Municipal and industrial waste disposal*. InTech, Croatia, pp 3–27
- Roberge PR (2000) *Handbook of corrosion engineering*. McGraw-Hill
- Rottger B, Kirsch R, Scheer W et al (2005) Multi frequency airborne EM surveys—a tool for aquifer vulnerability mapping. In: Butler DK (ed) *Near surface geophysics*. Society of Exploration Geophysicists, pp 643–651
- Singhal DC, Niwas S (1985) Aquifer transmissivity of porous media from resistivity data. *J Hydrol* 82:143–153
- Talabi AO, Kayode TJ (2019) Groundwater pollution and remediation. *J Water Resour Prot* 11:1–19. <https://doi.org/10.4236/jwarp.2019.111001>
- Thomas JE, George NJ, Ekanem AM et al (2020) Electrostratigraphy and hydrogeochemistry of hyporheic zone and water-bearing caches in the littoral shorefront of Akwa Ibom State University, Southern Nigeria. *Environ Monit Assess* 192:1–19
- Todd DK (1980) *Groundwater hydrology*, 2nd edn. Wiley, New York, p 535
- Ugwu SA, Nwosu JI (2009) Effect of waste dumps on groundwater using geophysical method. *J Appl Sci Manag* 13(1):85–89
- Ugwuanyi MC, Ibuot JC, Obiora DN (2015) Hydrogeophysical study of aquifer characteristics in some parts of Nsukka and Igbo Eze south local government areas of Enugu State, Nigeria. *Int J Phys Sci* 10(15):425–435
- Unicef (2006) *Progress for children. A report card on water and sanitation*. Issue 5
- WHO (2008) *Weekly epidemiological record*. WHO, Geneva, Switzerland 83(47):421–428
- WHO (2017) *Diarrhoeal disease: recommendations*, 2nd edn. WHO, Geneva, Switzerland
- Zohdy AAR, Eaton GP, Mabey DR (1974) *Application of surface geophysics to groundwater investigations*. United State Geophysical Survey, Washington, DC

**Publisher's Note** Springer Nature remains neutral with regard to jurisdictional claims in published maps and institutional affiliations.